Solid Earth Discuss., https://doi.org/10.5194/se-2018-43
Manuscript under review for journal Solid Earth
Discussion started: 31 May 2018

Soil erodibility estimation by using five methods of estimating *K* value: A case study in Ansai watershed of Loess Plateau, China

Wenwu Zhao, Hui Wei, Lizhi Jia, Stefani Daryanto, Yanxu Liu

State Key Laboratory of Earth Surface Processes and Resources Ecology, Faculty of Geographical Science, Beijing Normal University, Beijing 100875, China

Institute of Land Surface System and Sustainable Development, Faculty of Geographical Science, Beijing Normal University, Beijing 100875, China

Correspondence to: Wenwu Zhao (Zhaoww@bnu.edu.cn)

Abstract

The objectives of this work were to select the possible best texture-based method to estimate K and understand possible indirect environmental factors of soil erodibility. In this study, 151 soil samples were collected during soil surveys in Ansai watershed. Five methods of estimating *K* value were used to estimate soil erodibility, including the erosion-productivity impact model (EPIC), the nomograph equation (NOMO), the modified nomograph equation (M-NOMO), the Torri model and the Shirazi model. The *K* values in Ansai watershed ranged between 0.009 and 0.092 t ħm^2 ħr/(MJ ŧmm ħm^2). The *K* values based on Torri, NOMO, and Shirazi models were similar and were located close to each other in the Taylor diagrams. By combining the measured soil erodibility, we suggested Shirazi and Torri model as the optimal models for Ansai watershed. The correlations between soil erodibility and the selected environmental variables changed for different vegetation type. For native grasslands, soil erodibility had significant correlations with terrain factors. For most artificially managed vegetation types (e.g., apple orchards) and artificially restored vegetation types (e.g., sea buckthorn), the soil erodibility had significant correlations with the growing conditions of vegetation. The dominant factors that influenced soil erodibility differed with different vegetation types. Soil erodibility had indirect relationship

Solid Earth Discuss., https://doi.org/10.5194/se-2018-43
Manuscript under review for journal Solid Earth
Discussion started: 31 May 2018

with not only environmental factors (e.g., elevation and slope), but also human activities which potentially altered soil erodibility.

Keywords: Influencing factors, Soil erodibility, Variation features, Shirazi model, Torri model

1 Introduction

Soil erodibility (*K*), as one of the key factors of soil erosion (Igwe, 2003; Fu et al., 2005; Ferreira et al., 2015), is defined as the susceptibility of soil to erosional processes (Bagarello et al., 2012; Bryan et al., 1989). It has been extensively used in both theoretical and practical approaches to measure soil erosion. Yet it is a complex concept and is affected by many factors, including soil properties (e.g., soil texture, permeability and structural stability) (Chen et al., 2013; Wang et al., 2015; Manmohan et al., 2012); terrain (Wang et al., 2012; Mwaniki et al., 2015; Parajuli et al., 2015); climate (Hussein et al., 2013; Sanchis et al., 2010); vegetation (Sepúlveda-Lozada et al., 2009); and land use (Cerdà et al., 1998; Tang et al., 2016). In order to calculate soil erodibility, many strategies have been used to perform research to understand soil erodibility, including measurements of physical and chemical soil properties, instrumental measurements, mathematical models and graphical methods (Wei et al., 2017). Although a direct measurement of soil erosion with large plots under natural rainfall over long-term period can provide more accurate estimates of soil erodibility, this method is time consuming and very expensive (Bonilla et al., 2012; Vaezi et al., 2016a, b). Therefore, mathematical models are more commonly used to estimate soil erodibility.

Some of the most common estimation models are the nomogram model and the modified nomogram model, which were established by Wischmeier (Wischmeier et al., 1971, 1978); the erosion-productivity impact model (EPIC), which was developed by Williams (Williams et al., 1990); the best nonlinear fitting formula using the physical and chemical properties of the soil, which was developed by Torri (Torri et al., 1997); and the estimation model developed by Shirazi that is using the average size of the soil geometry (Shirazi et al., 1988).

Solid Earth Discuss., https://doi.org/10.5194/se-2018-43
Manuscript under review for journal Solid Earth
Discussion started: 31 May 2018

Each estimation method may differ in terms of their applicability, even within the same area because different estimation methods include different physical and chemical soil properties (Lin et al., 2017; Wang et al., 2013b; Kiani et al., 2016). Consequently, the estimated results can differ significantly because soil conditions vary by region (Lin et al., 2017; Wang et al., 2013b). Selecting the optimal estimation method of soil erodibility is therefore critical to estimate the amount of soil erosion.

Soil erosion in the Loess Plateau of China is among the highest in the world (Fu et al., 2009; Huang et al., 2016). The area affected by soil and water loss is as large as 4.5×10^5 km^2 (~71% of the local land area) and the long-term average sediment loss is up to 1.6×10^9 t (Fu et al., 2017). To maintain water quality and to control soil erosion (Fu et al., 2011), the Chinese government has implemented a large-scale policy to convert farmlands to forests and grasslands since the 20th century (Lü et al., 2012; Feng et al., 2013b; Wu et al., 2016). Although this large-scale introduction of vegetation should reduce soil erosion, the extent of the reduction remains unclear. Accordingly, different estimation methods should be used to calculate erosion factors, including soil erodibility factor. In this article, Ansai watershed in Loess Plateau of China was chosen as a case study, and the above five estimation methods of estimating *K* value were used, and the objectives of this study are (1) to estimate soil erodibility factor with different methods; (2) to select the possible best texture-based method to estimate *K*; (3) to understand possible indirect environmental factors on soil erodibility.

2 Materials and methods

2.1 Study area

The Ansai watershed (108°5′44″-109°26′18″E, 36°30′45″-37°19′3″N) is located in the upper reaches of the Yanhe River. This watershed lies in the northern part of Shanxi province and the inland hinterland of the northwestern Loess Plateau and at the edge of the Ordos basin. It belongs to the typical loess hilly-gully region and covers an area of approximately 1334 km^2. The topography is complex and varied, and the ground surface is

Solid Earth Discuss., https://doi.org/10.5194/se-2018-43
Manuscript under review for journal Solid Earth
Discussion started: 31 May 2018

fragmented. The elevations within the watershed are high in the northwest and low in the southeast, and these elevations range from 997 to 1731 m above sea level. The watershed belongs to the mid-temperate continental semi-arid monsoon climate region. The average annual precipitation is 505.3 mm, and 74 percent of the rainfall occurs from June to September. The predominant land use types in the Ansai watershed are rain-fed farmland, apple orchard, native grassland, pasture grassland, shrubland, and forest (Feng et al., 2013a). The soil type in this study area is loess soil with low fertility and high vulnerability to erosion (Zhao et al., 2012; Yu et al., 2015).

2.2 Sample point setting

The soil data used in this study came from 151 typical sample data sets that were obtained during soil surveys conducted from July to September in 2014. The soil types of all 151 sample points are loess soil. Representative vegetation were selected, which included (1) natural vegetation, including native grassland (NG); (2) artificially managed vegetation types, including apple orchards (AO) and farmland (FL); and (3) artificially restored vegetation types, including pasture grassland (PG), sea buckthorn (SB), *Caragana korshinskii* (CK), David's peach (DP), and black locust (BL). The distance between each vegetation sampling site was at least 2 km, the area of each vegetation type was greater than 30 m by 30 m, and the selected sample plots were distributed evenly within the study area. The sample plots within the farmland and grassland had a size of 2 m by 2 m, whereas the corresponding dimensions for the sample plots within the shrubland and forest areas were 5 m by 5 m and 10 m by 10 m, respectively. Each sample plot was repeated three times. The locations of the sampling points were determined using a GPS unit (Garmin eTrex 309X). The collected soil samples were taken back to the laboratory, dried naturally, ground and filtered with a 2-mm sieve. The grain size distributions of the soil samples were evaluated using the hydrometer method. The size classes of the particles in this study were as follows: sand (0.005-2.0 mm), silt (0.002-0.05 mm) and clay (< 0.002 mm).

To fully explore the primary factors influencing soil erodibility in the Ansai watershed, we chose four types

of environmental factors, including physicochemical soil properties, topographic factors, climate factors and vegetation factors. While soil erodiblity does not directly depend on environmental factors, soil properties such as soil particle and soil organic matter can be affected by environmental factors. Soil erodibility thus has indirect relationship with the environmental factors. These environmental factors covered 20 independent variables, specifically elevation (Ele), slope position (SP), slope aspect (SA), slope gradient (SG), slope shape (SS), clay (Cla) content, silt (Sil) content, sand (San) content, organic matter (OM) content, soil bulk density (SBD), porosity (Por), average annual rainfall (AAR), vegetation coverage (VC), aboveground biomass (AB), vegetation height (VH), litter biomass (LB), plant density (PD), crown (Cro), basal diameter (BD), and branch number (BN). All of the environmental factors were derived from the field surveys. The main characteristics and sampling numbers for the study area are shown in Table 1, and the sampling points are shown in Fig.1. Based on the results of the Spearman correlation analysis, we then retained some environmental variables that displayed significant correlations ($P < 0.05$) with soil erodibility to perform a principal component analysis (PCA) and to obtain the minimum data set (MDS) (Xu et al., 2008). Only principal components (PCs) with eigenvalues $N >$ 1.0 and only variables with highly weighted factor loadings (i.e., those with absolute values within 10% of the highest value) were retained for the MDS (Mandal et al., 2008).

2.3 Research methods

Soil erodibility indicates the degree of difficulty that soil becomes separated, eroded and transported by rainfall erosion (Wang et al., 2013a; Cerdà et al., 2017). Soil erodibility factor, which is commonly known as the *K*-factor in the model, is defined as the average rate of soil loss per unit of rainfall erosivity index from a cultivated continuous fallow plot on a 22.1-m-long, 9% slope in the universal soil loss equation (Zhang et al., 2008). To minimize bias from using only one estimation method, we estimated the *K* values using five estimation models (i.e., EPIC, NOMO, M-NOMO, Torri and Shirazi), that have been widely applied in the research on soil

Solid Earth Discuss., https://doi.org/10.5194/se-2018-43
Manuscript under review for journal Solid Earth
Discussion started: 31 May 2018

111 erodibility (Wischmeier et al., 1971, 1978; Williams et al., 1990; Torri et al., 1997; Shirazi et al., 1988).

112 *2.3.1 K value estimation using the EPIC model*

113 The erosion-productivity impact model (EPIC) developed by Williams (Williams et al. 1990) is as follows:

$$K = [0.2 + 0.3e^{-0.0256\,SAN\left(1-\frac{SIL}{100}\right)}]\left(\frac{SIL}{CLA+SIL}\right)^{0.3}\left(1.0-\frac{0.25C}{C+e^{3.72-2.95C}}\right)\left(1.0-\frac{0.7SN_1}{SN_1+e^{-5.51+22.9SN_1}}\right) \quad (1)$$

114 where *SAN* is the percent sand content, *SIL i*s the percent silt content, *CLA* is the percent clay content, *C* is the
115 percent organic carbon content, and SN_1 = 1-*SAN*/100. The resulting *K* value is reported in United States
116 customary units of [short ton ac ft / (100 ft short ton ac in)].

117 *2.3.2 K value estimation using the NOMO model*

118 Wischmeier (Wischmeier et al., 1971) proposed this model after analyzing the relationship between soil
119 erosion and five soil characteristic indicators, including the percent silt+very fine sand fraction (0.05-0.1 mm),
120 the percent sand fraction, the soil organic matter content, a code for soil structure, and a code for soil
121 permeability:

$$K = [2.1\times10^{-4}M^{1.14}(12-OM)+3.25(S-2)+2.5(P-3)]/100 \quad (2)$$

122 where *M* is the product of the percent of silt+very fine sand and the percent of all soil fractions other than clay,
123 *OM* is the soil organic matter content (%), *S* is the soil structure code, and *P* is the soil permeability code. The
124 resulting K value is reported in United States customary units of [short ton ac ft/(100 ft short ton ac in)].

125 *2.3.3 K value estimation using the M-NOMO model*

126 On the basis of the universal soil loss equation (USLE) model, the RUSLE model was modified for
127 calculating soil erodibility; that is, a revised nomograph equation was devised (Wischmeier et al., 1978) based on
128 the nomograph equation. The revised nomograph equation is:

$$K = [2.1\times10^{-4}M^{1.14}(12-OM)+3.25(2-S)+2.5(P-3)]/100 \quad (3)$$

129 where *M* is the product of the percent of silt+very fine sand and the percent of all soil fractions other than clay,

Solid Earth Discuss., https://doi.org/10.5194/se-2018-43
Manuscript under review for journal Solid Earth
Discussion started: 31 May 2018

130 *OM* is the soil organic matter content (%), *S* is the soil structure code, and *P* is the soil permeability code. The
131 resulting K value is reported in United States customary units of [short ton ac ħ/(100 ft short ton ac ·in)].

132 *2.3.4 K value estimation using the Torri model*

133 Torri (Torri et al., 1997) established this model in 1997 using data describing soil particle size and soil
134 organic matter content. The model has few parameters, and acquisition of the relevant data is simple. The
135 formula used in evaluating this model is as follows:

$$K = 0.0293(0.65 - D_g + 0.24D_g^{\ 2}) \times \exp\left\{-0.0021\frac{OM}{c} - 0.00037\left(\frac{OM}{c}\right)^2 - 4.02c + 1.72c^2\right\} \quad (4)$$

136 where *OM* is the percent content of soil organic matter, and *c* is the percent content of clay. In addition, the D_g
137 can be calculated by the following formula:

$$D_g = \sum f_i \lg\sqrt{d_i d_{i-1}} \quad (5)$$

138 where D_g is the Napierian logarithm of the geometric mean of the particle size distribution, d_i (mm) is the
139 maximum diameter of the *i*-th class, d_{i-1} (mm) is the minimum diameter and f_i is the mass fraction of the
140 corresponding particle size class. We calculate the D_g based on three particle size classes, namely sand, silt, and
141 clay. The resulting *K* values are reported in the international units of [(t ħm^2 ħ)/(MJ ·mm ħm^2)].

142 *2.3.5 K value estimation using the Shirazi model*

143 Shirazi (Shirazi et al., 1988) put forward a model that is appropriate for situations involving fewer physical
144 and chemical properties of the soil materials. He suggested that *K* values can be calculated through considering
145 only the geometric mean diameter (D_g) of the soil grains. The relevant formula is:

$$K = 7.594\left\{0.0034 + 0.0405\,e^{-\frac{1}{2}\left[\frac{\log(D_g)+1.659}{0.7101}\right]^2}\right\} \quad (6)$$

$$D_g(mm) = e^{0.01\sum f_i \ln m_i} \quad (7)$$

146 where D_g is the geometric mean diameter of the soil particles, f_i is the weight percentage of the *i*-th particle size

Solid Earth Discuss., https://doi.org/10.5194/se-2018-43
Manuscript under review for journal Solid Earth
Discussion started: 31 May 2018

fraction (%), m_i is the arithmetic mean of the particle size limits for the *i*-th fraction (mm), and *n* is the number of particle size fractions. The resulting *K* value is reported in United States customary units of [short ton ac ħ/(100 ft short ton ac in)].

To increase the comparability of the results from the different estimation models, our research adopted the international units for the *K* values, [t ħm^2 ħr/(MJ ħmm ħm^2)]. The international *K* value is equal to the *K* value reported in the United States customary units, multiplied by 0.1317.

To clarify the form of the distribution, we adopted the Kolmogorov-Smirnov test (Table 2) and made the frequency distribution figures of soil erodibility for each model (Fig. 2). The *P* value>0.05 showed that the *K* values obtained using the five methods were normally distributed. Therefore, the soil erodibility *K* values measured within the study area can be analyzed directly using statistical methods without data conversion (Fang et al. 2016).

2.3.6 K value comparisons

In order to discuss the possible best texture-based method to estimate *K*, related researches on K estimation, especially the measured value of K in Loess Plateau of China, have been collected. Taylor Diagram was also used to compare the difference between models.

3 Results

3.1 Soil erodibility based on five different models in Ansai watershed

We found that the descriptive statistics of the K values in Ansai watershed differed when different models were used (Table 2). The range of *K* values based on the five methods were between 0.032 and 0.060, 0.046 and 0.092, 0.047 and 0.088, 0.009 and 0.066, and 0.018 and 0.044 [t ħm^2 ħr/(MJ ħmm ħm^2)] for K_{EPIC}, K_{NOMO}, $K_{M\text{-}NOMO}$, K_{Torri}, and $K_{Shirazi}$ respectively. The range of the maximum values were 1.875, 2.000, 1.872, 7.333 and 2.444 times larger than the corresponding minimum values (Table 2). The differences between the mean and

Solid Earth Discuss., https://doi.org/10.5194/se-2018-43
Manuscript under review for journal Solid Earth
Discussion started: 31 May 2018

median values were 0.001, -0.001, 0.000, 0.000, and 0.000 [t ħm^2 ħr/(MJ ŧmm ħm^2)], respectively. The standard deviations (SDs) of the *K* values were 0.408, -0.447, -1.079, -2.639, and 0.059, respectively, and the skewnesses of the *K* values were 0.946, 0.956, 4.353, 16.872, and 0.009, respectively. The *Cv* value of $K_{M\text{-}NOMO}$ was 0.067 $<$ 10 %; in addition, the *Cv* values of K_{EPIC}, K_{NOMO}, K_{Torri}, and $K_{Shirazi}$ were 0.109, 0.110, 0.113, and 0.182, respectively, all of which were between 10 % and 100 %.

In the Taylor diagrams (Taylor, 2001) (Fig. 3), the *K* values based on EPIC model is used as the reference object. The *K* values based on Torri, NOMO, and Shirazi models were similar and were located close to each other. In contrast, there was inconsistency in the *K* values estimated by M-NOMO and EPIC models.

3.2 Spearman correlation coefficients between soil erodibility and environmental variables in Ansai watershed

The correlations between soil erodibility and the environmental variables varied with the different vegetation types (Table S1-S4). In general, soil erodibility in artificially managed vegetation types (apple orchards and David's peach) and artificially restored vegetation types (e.g., sea buckthorn and black locust) had significant correlation with vegetation properties. For example, soil erodibility in areas planted with apple orchards had a significant positive correlation with plant density (Table S1). The soil erodibility of areas with sea buckthorn had significant negative correlations with the slope gradient and plant density, whereas it had significant positive correlations with the average annual rainfall and aboveground biomass (Table S3). The soil erodibility of areas with David's peach had a significant positive correlation with the aboveground biomass, whereas it had significant negative correlations with the slope gradient, vegetation coverage, vegetation height, crown width and basal diameter (Table S4). The soil erodibility of areas with black locust had a significant negative correlation with the elevation, whereas it had significant positive correlations with the slope position, slope gradient, soil bulk density, vegetation coverage, litter biomass and branch number (Table S4). Meanwhile,

Solid Earth Discuss., https://doi.org/10.5194/se-2018-43
Manuscript under review for journal Solid Earth
Discussion started: 31 May 2018

soil erodibility in areas under different vegetation types such as grasslands or farmlands were more correlated with soil or landscape properties. The results of the correlation analysis between estimated *K* values and the selected environmental variables showed that soil erodibility in farmlands had significant positive correlations with the slope position, slope shape and average annual rainfall and displayed a significant negative correlation with the slope gradient (Table S1). Soil erodibility of areas with native grasslands had a significant negative correlation with the elevation, whereas it had significant positive correlations with the average annual rainfall and slope gradient (Table S2). Soil erodibility of areas with pasture grasslands did not have significant correlations with the environmental variables other than soil organic matter content and the soil particle size (Table S2). The soil erodibility of areas with *Caragana korshinskii* had a significant positive correlation with the elevation, whereas it had a significant negative correlation with the average annual rainfall (Table S3).

3.3 Principal component analysis of soil erodibility under different vegetation types

Our results showed the PCA identified one PC each for apple orchards, native grasslands, sea buckthorn, *Caragana korshinskii* and pasture grasslands, which accounted for 100%, 48.88%, 62.05% and 53.61 of the variances, respectively (Table S5). The PCA identified two PCs each for farmland and David's peach; the corresponding cumulative variances were 73.93 % and 81.07 %, respectively. For black locust, the PCA identified three PCs that accounted for 70.25 % of the variance (Table S5). In farmland, PC1 included two variables that had highly weighted factor loadings, the slope shape and slope position, and PC2 included only the slope gradient, which had a highly weighted factor loading. In apple orchards, the highly weighted factor loading was the plant density. In native grasslands, PC1 included two variables that had highly weighted factor loadings, including the slope gradient and elevation. The pasture grasslands had no variables with highly weighted factor loadings because it had no significant environmental variables except the soil particle size and soil organic matter. The highly weighted factor loadings in areas with sea buckthorn were the slope gradient, aboveground

Solid Earth Discuss., https://doi.org/10.5194/se-2018-43
Manuscript under review for journal Solid Earth
Discussion started: 31 May 2018

biomass and plant density. In areas planted with *Caragana korshinskii*, two variables had highly weighted factor loadings, including the average annual rainfall and elevation. In areas planted with black locust, the highly weighted factor loadings of PC1 were the slope position, elevation and litter biomass; for PC2, the slope gradient and soil bulk density had high factor loadings, whereas only vegetation coverage had a high weighted factor loading for PC3. In areas planted with David's peach, PC1 included three variables that had highly weighted factor loadings, specifically the crown width, vegetation height and vegetation coverage, whereas only the basal diameter had a high factor loading for PC2 (Table S5).

The MDS of the soil erodibility included six environmental variables for black locust, four for David's peach, three each for farmland and sea buckthorn, two each for native grasslands and *Caragana korshinskii*, one for apple orchards and none for pasture grasslands (Table 3). In addition to the soil organic matter and soil particle size, which are included in the *K* value estimation equations, the dominant factors affecting the soil erodibility for farmland were slope shape, slope gradient and slope position. For apple orchards, the only dominant factor affecting soil erodibility (except the soil organic matter and soil particle size) was plant density. For areas with native grasslands, the dominant factors affecting soil erodibility were soil organic matter, soil particle size, slope gradient and elevation. For areas with sea buckthorn, the dominant factors affecting soil erodibility were aboveground biomass, slope gradient and plant density in addition to the two soil properties. The dominant factors affecting soil erodibility in areas with *Caragana korshinskii* were soil particle size, soil organic matter, average annual rainfall and elevation. For areas with black locust, the dominant factors were the slope gradient, slope position, elevation, litter biomass, soil bulk density and vegetation coverage in addition to the soil organic matter and soil particle size. The dominant factors affecting soil erodibility in areas with David's peach included the soil organic matter, soil particle size, crown width, vegetation height and vegetation coverage.

4 Discussion

Solid Earth Discuss., https://doi.org/10.5194/se-2018-43
Manuscript under review for journal Solid Earth
Discussion started: 31 May 2018

235 **4.1 The optimal methods for estimating *K* values in Ansai watershed**

236 In this study, we found that different models resulted in different estimations of soil erodibility (Table 2).
237 Since different estimation methods use different soil attributes as input parameters; even if the input parameters
238 are the same, the decision coefficients of the same input parameters are different. For example, the EPIC model
239 focuses on the features of the soil particle and soil nutrients, while the NOMO model focuses on not only the soil
240 particle size and soil nutrient characteristics, but also the soil structure characteristics, such as soil structure code
241 and soil permeability code. The existing soil erodibility estimation equations are used to calculate soil erodibility
242 based on data on the physicochemical soil properties, such as soil texture, soil structure, soil permeability and
243 soil organic matter content (Wischmeier et al., 1971, 1978; Williams et al., 1990; Torri et al., 1997; Shirazi et al.,
244 1988). Among these factors, the main physical soil property is the soil particle composition, such as the contents
245 of sand, silt and clay, and the main chemical soil property is the soil organic matter content (Wei et al., 2017).

246 Our results showed that the *K* values based on Torri, NOMO, and Shirazi models were are located close to
247 each other in the Taylor diagrams (Fig.3) and those three models could therefore represent the soil erodibility in
248 Ansai watershed. Based on previous studies, these models have also been recommended as the optimal models in
249 Chinese subtropical zone, purple hilly region, Northeast China, and Chinese Loss Plateau (Table 4). We, however,
250 suggested Torri and Shirazi models as better representatives of the models, based on their estimated K values and
251 the actual (measured) soil erodibility data in Ansai watershed (Zhang et al., 2001; Table S6). The estimated *K*
252 value based on Torri and Shirazi models were closer to the measured soil erodibility data among the three
253 possible appropriate models (Table 2 and Table S6). Our suggestions were also supported by a study by Lin et al.
254 (2017) who showed that the estimated *K* value based on Torri and Shirazi models was closer to the measured
255 value.

256 **4.2 Environmental factors that influenced the soil erodibility**

Solid Earth Discuss., https://doi.org/10.5194/se-2018-43
Manuscript under review for journal Solid Earth
Discussion started: 31 May 2018

Based on the definition of K factor by Wischmeier et al. (1971), soil erodiblity is estimated by texture data, organic matter content, soil structure index, soil permeability index. While soil erodiblity does not directly depend on environmental factors, soil properties such as soil particle and soil organic matter can be affected by environmental factors. Soil erodibility thus has indirect relationship with the environmental factors, particularly vegetation type that influences the generation of soil organic matter and the composition of soil particle. Soil erodibility had different correlation with selected environmental variables, which resulted in changes in the dominant factors that influenced the soil erodibility (Tables S1-S5, Table 3). In native grasslands, soil erodibility had significant correlations with terrain factors (e.g., elevation, slope degree) (Table S1, Table S4), and the dominant factors influencing the soil erodibility were soil properties and topography. With the increase of elevation and slope, the physical and chemical soil properties (e.g., soil permeability, soil bulk density, and soil nutrient) and soil surface conditions are changed, further lead to the changes of soil particle size composition and soil erodibility (Zhao et al., 2015). For example, Li et al. (2011) found that the silt content was higher than sand in low than high elevations and Liu et al. (2005) found that slope gradient is negatively correlated with soil nutrients (e.g., soil organic matter, available nitrogen).

For most artificially managed vegetation types (apple orchards and David's peach) and artificially restored vegetation types (e.g., sea buckthorn and black locust), soil erodibility had significant correlations with the vegetation properties (Table S1, Table S3-S4). By changing the physicochemical soil properties and soil structure stability, vegetation properties could affect soil erodibility. For example, the dominant factor(s) influencing the soil erodibility associated with apple orchards was plant density, sea buckthorn was aboveground biomass, black locust were litter biomass and vegetation coverage, and David's peach were crown width, vegetation height, basal diameter and vegetation coverage (Table S1). Because all these vegetation types are more or less affected by human activities, soil erodibility can also indirectly be affected by vegetation recovery and land cover change.

Solid Earth Discuss., https://doi.org/10.5194/se-2018-43
Manuscript under review for journal Solid Earth
Discussion started: 31 May 2018

5 Conclusions

We evaluated soil erodibility using five estimation models in Ansai watershed; the estimated *K* values based on different models were different from one another and the resulting *K* values ranged between 0.009 and 0.092 t ħm^2 ħr/(MJ ŧmm ħm^2). Based on Taylor diagrams and previous studies, we considered Shirazi and Torri model the optimal models for Ansai watershed. Since soil erodibility is estimated by soil properties, soil erodibility has indirect relationship with environment factors, including elevation and slope degree, and to a lesser extent, human activities. By changing vegetation density, biomass, and cover, human can indirectly affect soil erodibility.

Acknowledgments This work was supported by the National Key Research Program of China (No. 2016YFC0501604), the National Natural Science Foundation of China (No.41771197), and the State Key Laboratory of Earth Surface Processes and Resource Ecology (No. 2017-FX-01(2)). We would like to thank Jing Wang, Xiao Zhang, Qiang Feng, Xuening Fang, Jingyi Ding, and Yuanxin Liu for their support and contributions during the fieldwork.

References

Bagarello, V., Stefano, C. D., Ferro, V., Giordano, G., Iovino, M., Pampalone, V.: Estimating the USLE soil erodibility factor in Sicily, south Italy, Appl. Eng. Agric., 28, 199–206, 2012.

Bonilla, C. A., Johnson, O. I.: Soil erodibility mapping and its correlation with soil properties in Central Chile, Geoderma, 189–190, 116-123, 2012.

Bryan, R. B., Govers, G., Poesenb, S. R. A.: The concept of soil erodibility and some problems of assessment and application, Catena, 16, 393–412, 1989.

299 Cerdà, A., Keesstra, S. D., Rodrigo-Comino, J., Novara, A., Pereira, P., Brevik, E., Gimenez-morera A,
300 Fernandez-raga M, Pulido M, Prima S D, Jordán, A.: Runoff initiation, soil detachment and connectivity
301 are enhanced as a consequence of vineyards plantations, J. Environ. Manage., 202, 268–275, 2017.
302 Cerdà, A.: Soil aggregate stability under different Mediterranean vegetation types, Catena, 32, 73–86, 1998.
303 Chen, X. Y., Zhou, J.: Volume-based soil particle fractal relation with soil erodibility in a small watershed of
304 purple soil, Environ. Earth Sci., 70, 1735–1746, 2013.
305 Fang, X. N., Zhao, W. W., Wang, L. X., Feng, Q., Ding, J. Y., Liu, Y. X., Zhang, X.: Variations of deep soil
306 moisture under different vegetation types and influencing factors in a watershed of the Loess Plateau,
307 China, Hydrol. Earth Syst. Sci., 20, 3309–3323, 2016.
308 Feng, Q., Zhao, W. W., Qiu, Y., Zhao, M. Y., Zhong, L. N.: Spatial heterogeneity of soil moisture and the scale
309 variability of its influencing factors: a case study in the Loess Plateau of China, Water, 5, 1226–1242,
310 2013a.
311 Feng, X. M., Fu, B. J., Lu, N., Zeng, Y., Wu, B. F.: How ecological restoration alters ecosystem services: an
312 analysis of carbon sequestration in China's Loess Plateau, Sci. Rep-UK., 3, 28–46, 2013b.
313 Ferreira, V., Panagopoulos, T., Andrade, R., Guerrero, C., Loures, L.: Spatial variability of soil properties and
314 soil erodibility in the Alqueva reservoir watershed, Solid Earth, 6, 383–392, 2015.
315 Fu, B. J., Liu, Y., Lü, Y. H., He, C. S., Zeng, Y., Wu, B. F.: Assessing the soil erosion control service of
316 ecosystems change in the Loess Plateau of China, Ecol. Complex., 8, 284–293, 2011.
317 Fu, B. J., Wang, S., Liu, Y., Liu, J. B., Liang, W., Miao, C. Y.: Hydrogeomorphic ecosystem responses to natural
318 and anthropogenic changes in the Loess Plateau of China, Annu. Rev. Earth Planet Sci., 45, 223–243, 2017.
319 Fu, B. J., Wang, Y. F., Lü, Y. H., He, C. S., Chen, L. D., Song, C. J.: The effects of land use combination on soil
320 erosion-a case study in Loess Plateau of China, Prog. Phys. Geog., 33, 793–804, 2009.

Fu, B. J., Zhao, W. W., Chen, L. D., Zhang, Q. J., Lü, Y. H., Gulinck, H., Poesen, J.: Assessment of soil erosion at large watershed scale using RUSLE and GIS: a case study in the Loess plateau of China, Land Degrad. Dev., 16, 73–85, 2005.

Huang, J., Wang, J., Zhao, X. N., Li, H. B., Jing, Z. L., Gao, X. D., Chen, X. L., Pute, W.: Simulation study of the impact of permanent groundcover on soil and water changes in jujube orchards on sloping ground, Land Degrad. Dev., 27(4), 946–954, 2016.

Hussein, M. H.: A sheet erodibility parameter for water erosion modeling in regions with low intensity rain, Hydrol. Res., 44, 1013–1021, 2013.

Igwe, C. A.: Erodibility of soils of the upper rainforest zone, southeastern nigeria, Land Degrad. Dev., 14, 323–334, 2003.

Kiani, F., Ghezelseflo, A.: Evaluation of soil erodibility factor(k) for loess derived landforms of Kechik watershed in Golestan Province, North of Iran, J. Mt. Sci-Engl., 13, 2028–2035, 2016.

Li, P., Li, Z. B., Zheng, Y.: Effect of different elevation on soil physical-chemical properties and erodibility in dry-hot valley, Bull. Soil Water Conserv., 31, 103–107, 2011. (in Chinese with English abstract).

Lin, F., Zhu, Z. L., Zeng, Q. C., An, S. S.: Comparative study of three different methods for estimation of soil erodibility K in Yanhe Watershed of China, Acta Pedologi Sinica., 54(5), 1136–1146, 2017. (in Chinese with English abstract).

Liu, S. L., Guo, X. D., Lian, G., Fu, B. J., Wang, J.: Multi-scale analysis of spatial variation of soil characteristics in Loess Plateau-case study of Hengshan County, J. Soil Water Conserv., 19, 105–108, 2005. (in Chinese with English abstract).

Lü, Y. H., Fu BJ, Feng X. M., Zeng, Y., Liu, Y., Chang, R. Y., Sun, G., Wu, B. F.: A policy-driven large scale ecological restoration: quantifying ecosystem services changes in the Loess Plateau of China, PLoS ONE, 7, 17–28, 2012.

Mandal, U. K., Warrington, D. N., Bhardwaj, A. K., Bar-Tal, A., Kautsky, L., Minz, D., Levy, G. J.: Evaluating impact of irrigation water quality on a calcareous clay soil using principal component analysis, Geoderma, 144, 189–197, 2008.

Mwaniki, M. W., Agutu, N. O., Mbaka, J. G., Ngigi, T. G., Waithaka, E. H.: Landslide scar/soil erodibility mapping using Landsat TM/ETM+ bands 7 and 3 normalised difference index: A case study of central region of Kenya, Appl Geogr., 64, 108–120, 2015.

Parajuli, S. P., Yang, Z., Kocurek, G.: Mapping erodibility in dust source regions based on geomorphology, meteorology, and remote sensing, J. Geophys. Res. Earth Surf., 119, 1977–1994, 2015.

Sanchis, M. P. S., Torri, D., Borselli, L., Poesen, J.: Climate effects on soil erodibility, Earth Surf. Proc. Land, 33, 1082–1097, 2012.

Sepúlveda-Lozada, A., Geissen, V., Ochoa-Gaona, S., Jarquin-Sanchez, A., dela-Cruz, S. H., Capetillo, E., Zamora- Cornelio, L. F., Revista, D. B. T.: Influence of three types of riparian vegetation on fluvial erosion control in Pantanos de Centla, Mexico, Rev. Biol. Trop., 57, 1153–1163, 2009.

Shirazi, M. A., Hart, J. W., Boersma, L.:A unifying quantitative analysis of soil texture: improvement of precision and extension of scale, Soil Sci. Soc. of Am. J., 52, 181–190, 1988.

Tang, F. K., Cui, M., Lu, Q., Liu, Y. G., Guo, H. Y., Zhou, J. X.: Effects of vegetation restoration on the aggregate stability and distribution of aggregate-associated organic carbon in a typical karst gorge region, Solid Earth, 7, 141–151, 2016.

362 Taylor, K.: Summarizing multiple aspects of model performance in a single diagram, J. Geophys. Res., 106,
363 7183–7192, 2001.
364 Torri, D., Poesen, J., Borselli, L.: Predictability and uncertainty of the soil erodibility factor using a global
365 dataset, Catena, 31, 1–22, 1997.
366 Vaezi, A. R., Abbasi, M., Bussi, G., Keesstra, S.: Modeling sediment yield in semi-arid pasture Micro
367 Catchments, NW Iran, Land Degrad. Dev., 28, 1274–1286, 2016b.
368 Vaezi, A. R., Hasanzadeh, H., Cerda, A.: Developing an erodibility triangle for soil textures in semi-arid regions,
369 NW Iran, Catena, 142, 221–232, 2016a.
370 Wang, A. J, Li, Z. G.: Spatial distribution of soil erodibility in Upper Yangtze River Region, Adv. Mater Res.,
371 610–613, 2944–2947, 2012.
372 Wang, B., Zheng, F. L., Römkens, M. J. M., Darboux, F.: Soil erodibility for water erosion: A perspective and
373 Chinese experiences, Geomorphology, 187, 1–10, 2013a.
374 Wang, B., Zheng, F. L., Römkens, M. J. M.: Comparison of soil erodibility factors in USLE, RUSLE2, EPIC
375 and Dg models based on a Chinese soil erodibility database, Acta Agr. Scand. B-S. P., 63, 69–79, 2013b.
376 Wang, G. Q., Fang, Q. F., Wu, B. B., Yang, H. C., Xu, Z. X.: Relationship between soil erodibility and modeled
377 infiltration rate in different soils, J. Hydrol., 528, 408–418, 2015.
378 Wei, H., Zhao, W. W., Wang, J.: Research process on soil erodibility, Chin. J. Appl. Ecol., 28, 2749–2759, 2017.
379 (in Chinese with English abstract).
380 Williams, J. R.: The erosion-productivity impact calculator (EPIC) model: A case history, Phil. Trans. R. Soc. B.,
381 329, 421–428, 1990.
382 Wischmeier, W. H., Johnson, C. B., Cross, B. V.: Soil erodibility nomograph for farmland and construction
383 sites, J. Soil Water Conserv., 26, 189–193, 1971.

Wischmeier, W. H., Smith, D. D.: Predicting rainfall erosion losses-a guide to conservation planning, United States. Dept. of Agriculture Handbook, 537, 1978.

Wu, L., Liu, X., Ma, X.: Application of a modified distributed-dynamic erosion and sediment yield model in a typical watershed of hilly and gully region, Chinese Loess Plateau, Solid Earth, 1–26, 2016.

Xu, X. L., Ma, K. M., Fu, B. J., Song, C. J., Liu, W.: Relationships between vegetation and soil and topography in a dry warm river valley, SW China, Catena, 75, 138–145, 2008.

Yu, Y., Wei, W., Chen, L. D., Yang, L., Jia, F. Y., Zhang, H. D.: Responses of vertical soil moisture to rainfall pulses and land uses in a typical loess hilly area, china, Solid Earth, 6(2), 595–608, 2015.

Zhang, K. L., Shu, A. P., Xu, X. L., Yang, Q. K., Yu, B.: Soil erodibility and its estimation for agricultural soils in China, J. Arid Environ., 72, 1002–1011, 2008.

Zhao, M. Y., Zhao, W. W., Liu, Y. X.: Comparative analysis of soil particle size distribution and its influence factors in different scales: a case study in the Loess hilly-gully area, Acta Ecolgica Sinica, 35, 4625–4632, 2015. (in Chinese with English abstract).

Zhao, W. W., Fu, B. J., Chen, L. D.: A comparison between soil loss evaluation index and the C-factor of RUSLE: a case study in the Loess Plateau of China, Hydrol. Earth Syst. Sci., 16, 2739–2748, 2012.

Solid Earth Discuss., https://doi.org/10.5194/se-2018-43
Manuscript under review for journal Solid Earth
Discussion started: 31 May 2018

400 **Table 1** Landscape and soil characteristics in the study area

Vegetation types	Natural vegetation	Artificially managed vegetation		Artificially restored vegetation				
	NG	FL	AO	PG	SB	CK	BL	DP
Sampling number	25	22	10	11	15	18	38	12
Ele (m)	1392.60	1380.14	1370.10	1401.00	1435.67	1350.61	1326.54	1377.58
SG (°)	16.72	6.27	19.90	11.91	16.40	17.56	27.24	24.17
Cla (%)	7.44	7.93	7.05	7.88	6.70	7.21	8.30	8.34
Sil (%)	45.08	52.63	48.57	42.73	45.05	48.08	51.75	49.69
San (%)	47.48	39.44	44.38	49.39	48.25	44.71	39.95	41.97
OM (g/kg)	7.04	5.31	5.75	6.30	8.91	13.30	8.10	5.99
SBD (g/cm^3)	1.26	1.29	1.25	1.28	1.23	1.26	1.23	1.26
Por (%)	0.48	0.46	0.48	0.47	0.48	0.49	0.49	0.49
AAR (mm)	473.99	479.01	479.85	471.75	476.44	474.66	474.43	472.58
VC (%)	57.36	53.14	39.70	67.82	66.07	46.28	59.58	33.75
AB (g/m^2)	28.96	95.61	12.24	73.56	28.59	45.63	23.92	16.20
VH (m)	0.59	1.83	3.58	0.67	2.16	1.81	11.49	3.02
LB (g/m^2)	15.70	—	8.64	12.06	25.10	34.05	72.50	14.44
PD (/m^2)	—	—	30.50	—	262.40	131.89	58.66	36.17
Cro (cm)	—	—	398.39	—	184.85	205.20	448.72	293.40
BD (cm)	—	—	6.32	—	3.76	1.59	10.16	4.98
BN	—	—	10.17	—	—	27.88	12.86	8.13

401 Annotation: NG refers to native grassland, AO refers to apple orchard, FL refers to farmland, PG refers to pasture grassland, SB refers to sea
402 buckthorn, CK refers to *Caragana korshinskii*, DP refers to David peach, BL refers to black locust, Ele refers to elevation, SP refers to slope position,
403 SA refers to slope aspect, SG refers to slope gradient, SS refers to slope shape, Cla refers to clay, Sil refers silt, San refers to sand, OM refers to
404 organic matter, SBD refers to soil bulk density, Por refers to porosity, AAR refers to average annual rainfall, VC refers to vegetation coverage, AB
405 refers to aboveground biomass, VH refers to vegetation height, LB refers to litter biomass, PD refers to plant density, Cro refers to crown, BD refers to
406 basal diameter, BN refers to branch number.
407

Solid Earth Discuss., https://doi.org/10.5194/se-2018-43
Manuscript under review for journal Solid Earth
Discussion started: 31 May 2018

408 **Table 2** Statistics of soil erodibility in the Ansai watershed

Methods	Samples	Mean	Max	Min	Median	SD	Skew	Kurt	*Cv*	P
EPIC		0.046	0.060	0.032	0.045	0.005	0.408	0.946	0.109	1.102
NOMO		0.073	0.092	0.046	0.074	0.008	-0.447	0.956	0.110	0.775
M-NOMO	151	0.075	0.088	0.047	0.075	0.005	-1.079	4.353	0.067	0.910
Torri		0.053	0.066	0.009	0.053	0.006	-2.639	16.872	0.113	1.871
Shirazi		0.033	0.044	0.018	0.033	0.006	0.059	0.009	0.182	1.017

409 Annotation: EPIC refers to the erosion-productivity impact model, NOMO refers to the nomograph equation, M-NOMO refers to the modified
410 nomograph equation, Torri refers to the *K* value estimation model established by Torri, Shirazi refers to the *K* value estimation model established by
411 Shirazi, SD refers to the standard deviation, Skew refers to the Skewness, Kurt refers to the kurtosis, *Cv* refers to the coefficient of variation, and P
412 referes to p-value of Kolmogorov-Smirnov test.

413

Solid Earth Discuss., https://doi.org/10.5194/se-2018-43
Manuscript under review for journal Solid Earth
Discussion started: 31 May 2018

414 **Table 3** Principal component analysis (PCA) of environmental attributes

Vegetation types	Main influencing factors
Farmland	SS, SP, SG
Apple orchard	PD
Native grasses	SG, Ele
Pasture grasses	—
Sea buckthorn	AB, SG, PD
Caragana korshinskii	AAR, Ele
Black locust	SG, SP, Ele, LB, SBD, VC
David peach	Cro, VH, BD, VC

415 Annotation: SS refers to slope shape, SP refers to slope position, SG refers to slope gradient, PD refers to plant density, Ele refers to elevation, AB
416 refers to aboveground biomass, AAR refers to average annual rainfall, LB refers to litter biomass, SBD refers to soil bulk density, VC refers to
417 vegetation coverage, Cro refers to crown, VH refers to vegetation height, BD refers to basal diameter.
418
419

Solid Earth Discuss., https://doi.org/10.5194/se-2018-43
Manuscript under review for journal Solid Earth
Discussion started: 31 May 2018

420 **Table 4** Suggested soil erodibility estimation models in China

Study area	optimal models	References
Hilly area of Chinese subtropical zone	Torri	Zhang et al.,2009
Purple hilly region in Sichuan Basin	EPIC and NOMO,	Shi et al.,2012
typical black soil region in Northeast China	EPIC and NOMO,	Wang et al.,2012
Hilly and gully area of Chinese Loss Plateau	Torri and Shirazi	Lin et al., 2017
Hilly and gully area of Chinese Loss Plateau	Shirazi	Wei et al., 2017

421

422

Solid Earth Discuss., https://doi.org/10.5194/se-2018-43
Manuscript under review for journal Solid Earth
Discussion started: 31 May 2018

423 **Fig. 1** Location of the study area and the sampling points

424 **Fig. 2** Frequency distributions of soil erodibility

425 **Fig. 3** Taylor diagram were used to compare the estimating K values

426

Solid Earth Discuss., https://doi.org/10.5194/se-2018-43
Manuscript under review for journal Solid Earth
Discussion started: 31 May 2018

427 Figure 1

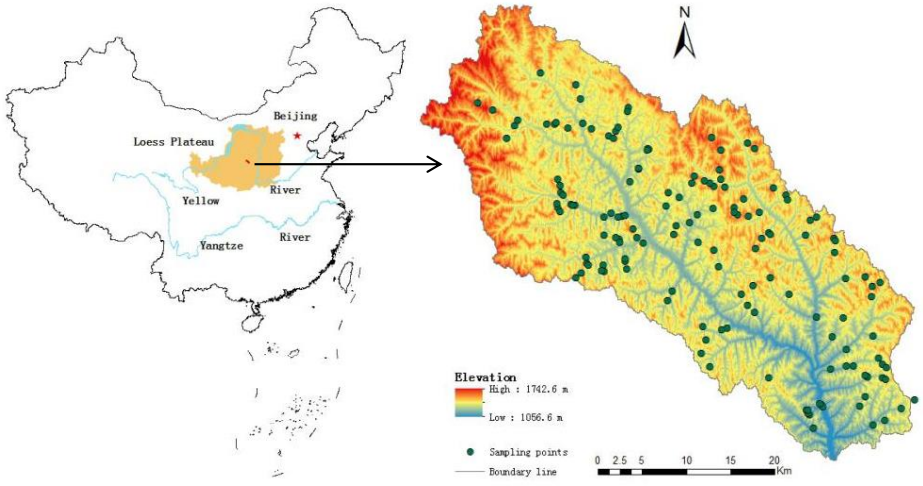

428

429

Solid Earth Discuss., https://doi.org/10.5194/se-2018-43
Manuscript under review for journal Solid Earth
Discussion started: 31 May 2018

Figure 2

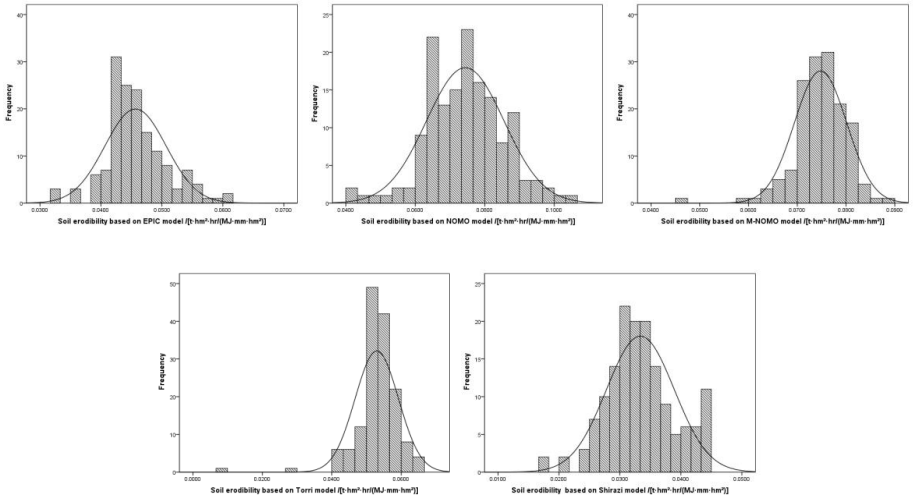

Solid Earth Discuss., https://doi.org/10.5194/se-2018-43
Manuscript under review for journal Solid Earth
Discussion started: 31 May 2018

434 Figure 3

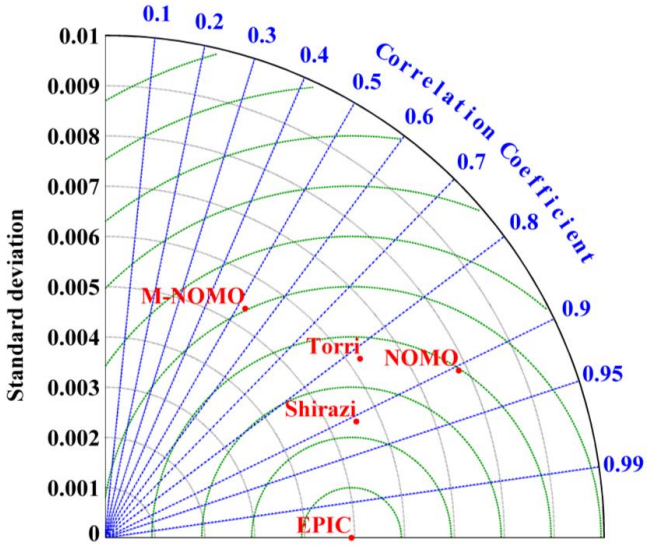

435